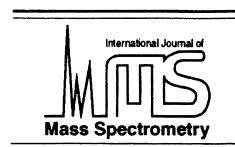




ELSEVIER

International Journal of Mass Spectrometry 207 (2001) 97–110



Swarm experiment on ionized water clusters

Tomasz Wróblewski^a, Emil Gazda^{a,b}, Jadwiga Mechlińska-Drewko^b,
Grzegorz P. Karwasz^{c,*}

^a*Institute of Physics, Pedagogical University, Arciszewskiego 22, 76-200 Słupsk, Poland*

^b*Faculty of Applied Physics and Mathematics, Gdańsk Technical University, Narutowicza 11/12, 80-952 Gdańsk, Poland*

^c*Istituto Nazionale per la Fisica della Materia, Dipartimento di Fisica, Università di Trento, 38050 Povo (TN), Italy*

Received 17 July 2000; accepted 22 December 2000

Abstract

Drift of positively ionized water clusters formed in a low-pressure electrical discharge was studied by mass spectroscopy. Ions $H^+(H_2O)_n$ with $n = 1-7$ were observed at room temperature and at pressures in a few hundreds Pa range. Relative cluster abundances depend on the reduced electrical field in the drift chamber. The $H^+(H_2O)_4$ clusters are somewhat more abundant than those with $n = 3, 5$. Fragmentation energies, in a rough agreement with other experimental and theoretical values, have been derived from equilibrium conditions for relative cluster abundances. Calculations of dissociation energies of cationic clusters with n up to 7 have been performed in Hartree-Fock approximation with a 6-311**G basis set. (Int J Mass Spectrom 207 (2001) 97–110) © 2001 Elsevier Science B.V.

Keywords: Water; Cations; Clusters; Dissociation

1. Introduction

The tendency of water molecules to form clusters is responsible for a number of chemical and physical phenomena. Some of these phenomena, as, for example, an anomalous thermal expansion coefficient $<4^\circ\text{C}$, are still not fully explained theoretically [1,2]. In chemistry, the formation of ionized aggregates $H^+(H_2O)_n$ containing few water molecules, that is, the hydration of proton, influences greatly the dissociation and transport processes in aqueous solutions [3–5]. Ionized water clusters also have been observed in the gaseous phase: in electrical discharges in moist air [6–8], in ambient air humidified by boiling water [9], and in the stratosphere

[10,11]. The importance of ionized clusters for the water vapor condensation is recognized [12]; their presence influences chemical reactions in Earth's atmosphere [13,14]. The proton transfer from the H_3O^+ ions has found large applications in a new generation of high-sensitivity mass spectrometers [15].

The recent experimental investigations concentrate on spectroscopic properties of water clusters [16,17]. However, the stability and geometrical configurations of both neutral and ionized clusters are still subject to intense theoretical discussions [18–22]. Essentially, three laboratory methods are used to form ionized water clusters: first, a free jet expansion of the water vapor ionized in external electrical discharge [16,23,24]; second, electron- [25,26] and photon- [17,27] impact ionization of neutral water cluster jets; and third, high-energy ion sputtering of ice surface

* Corresponding author. E-mail: karwasz@science.unitn.it

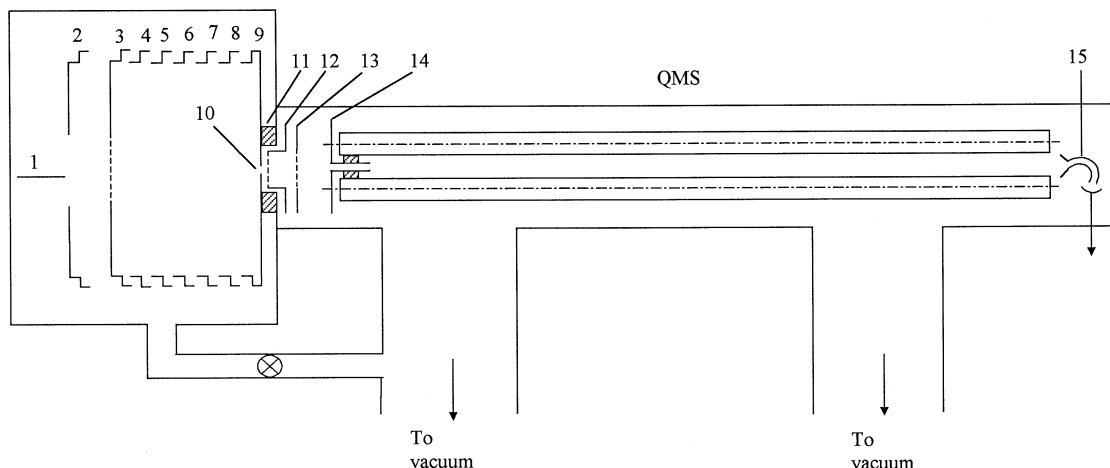


Fig. 1. Experimental set-up: electrodes 1 and 2, ion source; 3, tungsten grid; 4–9, guard electrodes; 3–9, drift region; 10, pinhole; 11, insulator; 12 and 13, grids; 14, grounded electrode; 15, channel electron multiplier; QMS, quadrupole mass spectrometer.

[28–31] or field ionization of liquid water [26]. A common feature of these experiments is that formation of clusters takes place at rather high pressures, during the supersonic expansion (and consequent cooling), in the presence of a buffer ionized gas or in a condensed phase. These physical conditions are different from those in the middle stratosphere (at ~ 45 km), where the water clusters dominate in the ionic composition, with temperatures up to 0°C and pressures in the 100-Pa range [11].

In this article, we report experimental studies of water clusters formed in the electrical discharge under low (in the 100-Pa range) pressure and drifting in a uniform, low-intensity electrical field. Relative abundances of positive clusters $\text{H}^+(\text{H}_2\text{O})_n$ with $n \leq 7$ are registered, and approximate binding energies are roughly estimated. This experiment can be defined as a swarm one [32], that is, one in which reacting species undergo multiple collisions and their populations are in a dynamic equilibrium. The Hartree-Fock *ab initio* method is used to evaluate the stability and dimensions of clusters. Partial results of this experiment have been presented elsewhere [33].

2. Experimental

The experimental set-up is a modified version of an apparatus used in the past for studies of water ion

mobility [34]. A schematic diagram of the apparatus is shown in Fig. 1. Briefly, it consists of two parts that are differentially pumped: a discharge region with the drift cell kept inside the vacuum vessel of $\sim 10\text{ dm}^3$ and a quadrupole mass spectrometer in a separate 50-cm-long vacuum tube. The two regions are separated by a stainless steel diaphragm with a 0.2-mm pinhole. The pumping system consists of two diffusion pumps of 100 l/s output filled with Santovac low-pressure oil. Butterfly valves above the diffusion pumps and a separate line for forevacuum pumping are used. The diffusion pumps are equipped with liquid nitrogen traps; however, we did not use them in measurements on water. The system is baked out before each cycle of measurements. The ultimate pressure in the system is 7×10^{-5} Pa. The pressure in the second (quadrupole mass spectrometer) chamber does not exceed 10^{-5} Pa, with the highest measurement pressures in the first part.

The ion source is defined by electrodes 1 and 2. The cathode made of a stainless steel pin is ~ 1 cm distant from the plane of the anode. Two types of discharge are used alternatively. The DC discharge is stabilized passively by an external resistance in series; the typical voltages of the discharge are between 200 and 600 V, and the current is ~ 0.1 – 0.3 mA, depending on the gas pressure. The high-frequency (HF) discharge is maintained by a 10-MHz sine generator

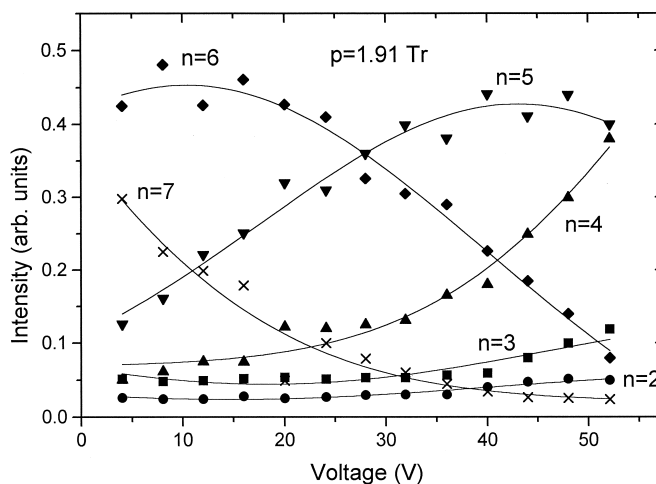


Fig. 2. Typical dependence of relative cluster populations at variable voltage and a constant pressure in the drift chamber.

enveloped by 100–1000-Hz square pulses. A few Watts of power are delivered to the discharge from the HF generator; as the impedance coupling is somewhat critical in our set-up, we do not measure the exact value of the HF power supplied.

The drift region extends between electrode 3 and electrode 9. The grid on electrode 3, three wires per millimeter on both sides of the electrode, is made of 0.05-mm-diameter tungsten with an evaporated gold layer on it; we proved that such a grid prevents the electric field from the discharge region from penetrating into the drift chamber. Seven equidistant electrodes in the drift region, made of stainless steel, have an 8.5-cm inner diameter. A constant field gradient from an external potential divider is applied to these electrodes. A weak accelerating voltage (the same as between the electrodes of the drift region) is applied between electrodes 2 and 3; however, in this region some electrical field penetration from the discharge is still present. Typical pressures in the drift chamber, as evaluated by an absolute membrane meter (Barocel 600, Edwards), are between 0.1 and 3×10^2 Pa.

After the drift chamber, in the second (low-pressure) region, the ions are accelerated by 50–200 V potential differences (between electrodes 10 and 14) and injected into the quadrupole spectrometer. The entrance of the spectrometer is kept on ground potential (electrode 14 in Fig. 1). The injection optics

contain an additional, two-element electrostatic lens (electrodes 12 and 13). The potentials on these lens elements are set between 0 and the full accelerating voltage. In the HF measurement series, the voltages on the exit electronic optics were adjusted in order to maximize the ion signal. In the DC series, we kept a constant accelerating voltage of 170 V and constant potentials on the focusing elements. In this way, we maintained a constant (for a given cluster) time of flight outside the drift chamber. The flight path from the exit of the drift chamber up to the detector was 45 cm. For a 170-V voltage applied to the zoom element, the flight times were typically between 10^{-5} and 10^{-4} s, depending on the mass of the cluster. Applied voltages are to be considered weak, that is, not influencing the clusters' structure. A channeltron electron multiplier with a low work function is used as ion detector.

In measurements using the HF discharge, a signal of ionized clusters was detected down to as low as a 4-V voltage on the drift chamber. This allowed us to observe clusters up to $n = 7$ at high pressures (in a few hundreds Pa range; see Fig. 2). In the case of the DC discharge, the absolute intensity of the signal was lower and not clearly measurable below a certain value of the voltage in the drift chamber. Therefore, presented results that start from 30 Td ($= 10^{-21}$ Vm²)

for the HF discharge and only 150 Td for the DC discharge; for details, compare Figs. 3(a) and 3(b).

The water-vapor flux was controlled by a high-precision needle valve. The temperature of the water container was kept 10 °C higher than the rest of the apparatus; this allowed us to maintain a good stability of pressure inside the drift chamber. The water container was degassed by several thaw-freeze cycles. All measurements were performed at room temperature (25 °C), which was kept constant within 2 °C. Mass spectra were registered for given drift (pressure, voltage) conditions within a few minutes' time. Runs affected by some instabilities (e.g., discharge conditions) were excluded from further analysis.

3. Relative abundances

In spite of a great number of experiments on formation of ionized water clusters (e.g., [23–32,35–47]), only in very few of them [29,35,41] were relative abundances for a wide range of sizes, starting from $n = 1$ (H_3O^+), reported. Extended mass spectra are available for heavy clusters [9,26,39–41]. For light clusters, scarce data exist, and they usually concentrate on selected clusters, such as $1 < n < 4$ [37,42,45,46] or $3 < n < 7$ [38].

The possibility of detecting different clusters in the same experiment depends on the ionizing agent: electron impact [35,44–46], proton impact [35], or electrical discharge [6,16,24,41]. Electrical discharges favor formation of a wider range of cluster sizes (see [41]). However, in order to facilitate the ionization [8], the thermalization of ions and the collisional stabilization of water clusters [37], buffer gases, or admixtures are frequently used, such as CH_4 [37,45,46], Ar [35], C_3H_8 [45]; for details, compare Table 1. Therefore, the measured relative abundances of the clusters formed in the discharges depended strongly on the gas pressure and on its composition, on the geometry and on the type of the discharge [6–8,23,36].

In this experiment (in a pure water vapor), we observe that with changing the discharge type (HF vs. DC) and its conditions, the absolute ion current at the

collector varies but the relative abundances for a given pressure and electrical field remain constant within the experimental error. On the contrary, the electrical field strength in the drift chamber influences not only the total ion current but also the relative abundances. It proves that the observed populations are determined by processes of clusters' formation and decay during the drift in the collision chamber and not by the discharge conditions itself.

A typical dependence of the relative cluster abundances versus the voltage applied in the drift chamber at a constant pressure is shown in Fig. 2 (for the HF discharge conditions). At low electrical fields, clusters with n ranging from $n = 2$ to $n = 7$ can be detected simultaneously. With rising the electrical field, heavier clusters ($n = 6, 7$) disappear, and the abundances of $n = 3, 4$ grow. In the mass spectra recorded at low pressures ($\cong 50$ Pa) and high voltages (250 V), only H_3O^+ ions were detected, together with traces (5%) of $\text{H}^+(\text{H}_2\text{O})_2$.

We note that these dependencies on the pressure and applied voltage can be normalized, in analogy to electron swarm experiments [48], by using the reduced (E/N , with N being molecule density) values of the electrical field. The physical meaning of this normalization is to refer the action of the external field to a single drifting particle [32,48].

The relative abundances for the HF and DC discharge versus the reduced electric field are shown in Figs. 3(a) and 3(b), respectively. In this figure, separate points represent relative abundances obtained in measurements at different pressures; all the points for a given cluster form the same smooth curve. (Only selected points obtained at different pressures are presented for clarity). The characteristic points of the abundance curves (thresholds for comparison of given clusters, values of E/N for equilibrium conditions between n and $[n - 1]$ clusters, the magnitudes of maxima) are the same within 10% for both types of discharges.

We are not aware of similar experimental curves. Present data resemble to some extent model abundance curves deduced from a thermodynamic experiment by Kebarle et al. [35]; see insert in Fig. 3(a). For example, at 250 Pa and in the limit of 0 Td

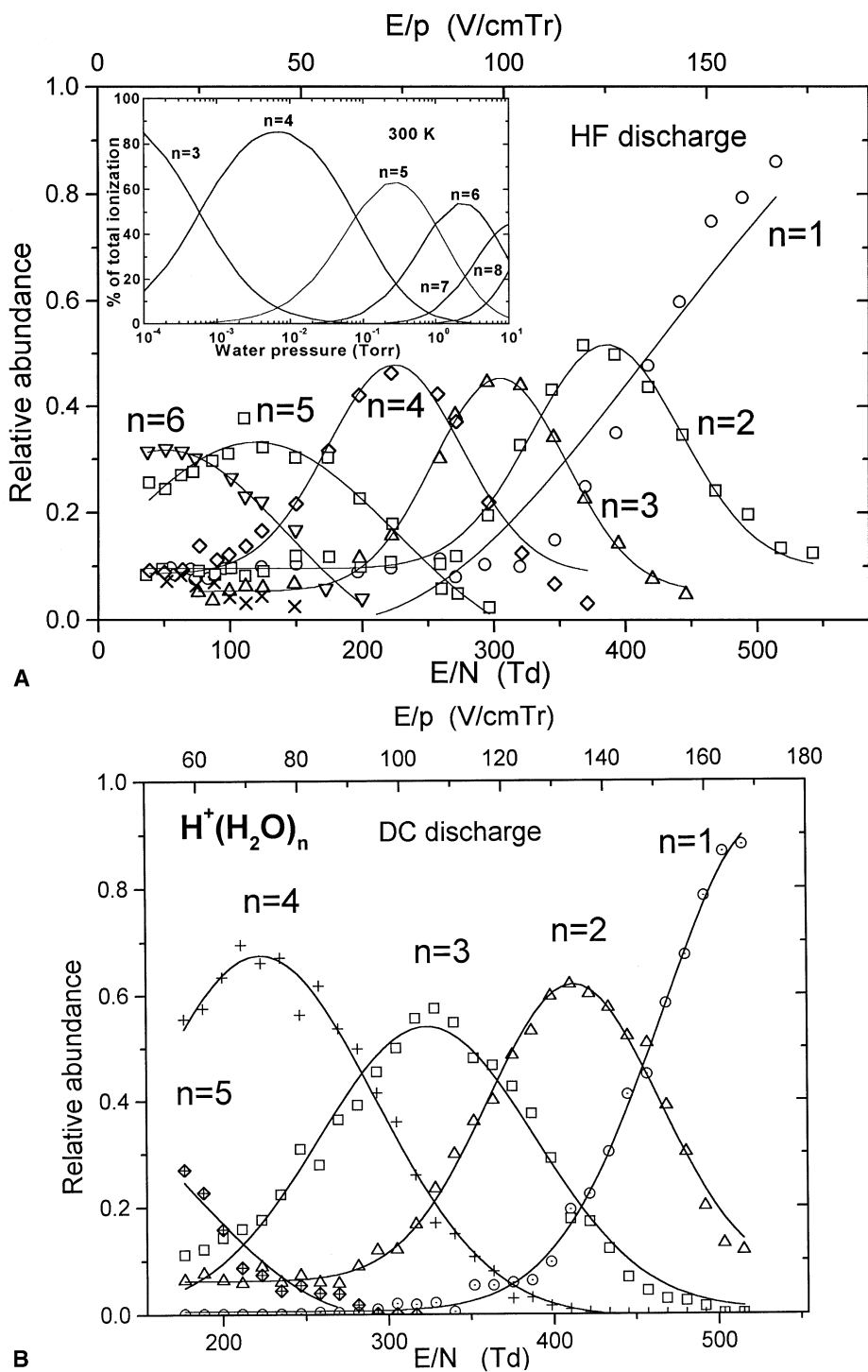


Fig. 3. Relative abundances of positive ions of water clusters versus reduced electrical field (HF discharge and DC discharge for *a* and *b*, respectively). Experimental points have been approximated by Gaussian curves plus, for certain *n*, a constant background. Insert in *a*: relative abundances as modelled by Kébarle et al. [35] from their thermodynamic measurements.

Table 1a

Enthalpies of formation (ΔH , in kcal/mol) and binding energies (ΔE , in kcal/mol) of small, hydrated-proton clusters (experimental values)

n , $n - 1$	ΔH (kcal/mol)							ΔE (kcal/mol)				
	Keb67	Cun72 <i>Lau82</i>	Beg71 (CH ₄)	Beg71 (C ₃ H ₈)	Meo77	Meo86	Hir86	Hon92	Hon93	Shi93	Mag91	Present
2,1	36	31.6	7	16.3	33.0 ^a	31.8	35.0	38.0	37.4		30	30.1
3,2	22.3	19.5	13	14.8	21.0	19.0	20.2	20.8	22.2		22	21.8
4,3	17	17.5	16.8	17.6	16.0	17.6		16.7	17.9		18	15.8
5,4	15.3	12.7	12.9			11.5					8.2	9.8
6,5	13	11.6	8.5							16.4	8.2	5.2
7,6	11.7	10.7								12.3	6.7	
8,7	10.3									10.0	6.7	

Keb67 [35], high-pressure mass spectroscopy, variable temperature ion source, Ar major gas; Cun72 [37], high-pressure mass spectroscopy, variable temperature ion source; Lau82 [38], high-pressure mass spectroscopy, variable temperature ion source; Beg71 [45], high-pressure mass spectroscopy, variable temperature, CH₄ major gas; Beg71 [45], high-pressure mass spectroscopy, variable temperature ion source, C₃H₈ major gas; Meo77 [42], high-pressure mass spectroscopy, variable temperature ion source, 1% H₂O in CH₄; Meo86 [44], high-pressure mass spectroscopy, variable temperature, 0.1–20% H₂O in CH₄; Hon92 [59], energies of solvation at 298 K from charge transfer reactions with CH₃CN; Hon93 [60], energies of solvation at 298 K from charge transfer reactions with CH₃CN; Mag91 [31], photodissociation of clusters from ion-sputtered ice.

^a $E_a = 29.8$ kcal/mole, the activation energy for the decomposition of the H(H₂O)₂⁺ complex in collisions with the buffer gas (CH₄) obtained from the experimental enthalpy.

electrical field, we observe dominating $n = 6$ clusters together with $n = 5, 7$; see Fig. 2, similarly observed by Kebarle et al. [35] at the same pressure. In both experiments, the maxima of relative abundances become lower with rising n .

Therefore, we note some differences. The most important one is the abscissa scale: $\log(p)$ in the experiment of Kebarle et al. and E/N in our case. This difference reflects different mechanisms of cluster

formation: agglomeration favored by the rise of pressure in the postionization free thermal-motion in [35], and a collisional formation and/or disintegration during the forced drift in the present set-up. Second, even in the limit of low electrical fields, we observe some non-zero populations of lighter clusters ($n \leq 4$ at 250 Pa, see Fig. 2), which differs from what has been reported by Kebarle et al. [35]. This effect is caused by a non-Maxwellian (epithermic) energy distribution

Table 1b

Theoretical binding energies (ΔE_D in kcal/mol) of small hydrated-proton clusters

n , $n - 1$	$-\Delta E_D$ (kcal/mol)						
	New77	Dea86	Hir86	Fri86	Present 4-31	Present 6-31G**	Present 6-311G**
1,0	179.5 ⁱ	183.2		171.4	183.2	179.9	178.8
2,1	37	43.6	35.0	34.4	43.9	33.9	33.7
3,2	26	30.9	20.2		31.2	25.0	25.0
4,3	22	26.1			25.8	20.3	21.0
5,4	16				18.7	14.0	13.5
6,5	15				13.4	13.3	12.9
7,6						10.9	11.2

New77 [57], Hartree-Fock in 4-31G basis set with the zero-energy correction from spectroscopic data; Hir86 [46], Hartree-Fock in 4-31G basis set with no zero-energy correction; Dea86 [66], Hartree-Fock in 3-21G basis set for geometry and 4-31G for dissociation energies with no zero-energy correction; Fri86 [68], fourth-order Møller-Plesset theory with triple-split valence polarisation basis 6-311**G(3df, 3pd) without zero-energy correction; Present, Hartree-Fock in specified basis sets and no zero-energy correction.

of clusters in the swarm [32]. Finally, in our abundances some maxima ($n = 4$) are higher than the neighboring ones ($n = 3, 5$), see Fig. 3(a). A similar effect was reported by Kebarle et al. [35], but only for the ion populations at 400 K (the insert in Fig. 3[a] has been calculated for 300 K).

4. Magic numbers

Present measurements indicate that formation of some cationic configurations is more favored than that of others. This observation is essentially the same for both types of discharge. In particular, the odd-number clusters, $n = 3, 5$ are slightly less abundant than the even-numbered ones, $\text{H}^+(\text{H}_2\text{O})_n$, $n = 2, 4, 6$ clusters. The relative differences are rather small; the abundance of the $n = 4$ cluster is somewhat 20% higher than the value obtained from the interpolation between $n = 3, 5$ maxima; see Fig. 3(b). The peak for $n = 6$ is at the edge of our E/N range, but also, in this case, the maximum is not lower than that for $n = 5$; see Fig. 3(a).

The enhanced stability of the $\text{H}^+(\text{H}_2\text{O})_4$ cluster has been the subject of a long-lasting discussion. It was first postulated by Eigen [3,4] that the H_3O^+ ion in liquid water is symmetrically surrounded by three other water molecules, each of them being equivalent; the $\text{H}^+(\text{H}_2\text{O})_4$ was considered to be a “brick” structure for the solvation of proton. Hardly any “magic” numbers for light cation clusters can be deduced from thermodynamic experiments [35,37–38,42–44]. Magic numbers were observed most clearly for negative ions $(\text{H}_2\text{O})_n^-$, with $n = 2, 6, 7$ [28,49,50] and for heavy cations $\text{H}^+(\text{H}_2\text{O})_n$, with $n = 21, 28, 33$ [23–26,50–51].

Analyzing in detail the different ways of producing ionized clusters, we note that agglomerates up to $n = 50$, with dominating $n = 4$ and $n = 1$ sizes, were observed in studies of ice sputtering by He^+ ions [29]. Enhanced intensities for $n = 4$ were seen in electro-spray spectra of water [39], in field ionization of water droplets [26], and in electron ionization of $\text{CH}_4/\text{H}_2\text{O}$ mixtures [52]. A clear maximum at $n = 4$ was

observed in studies of the pickup of water molecules by NO-ionized clusters [53].

No preferred configurations were observed in studies of the photoionization of neutral water clusters present in a supersonic water vapor stream [27]; the relative intensities in the published mass spectrum descend monotonically from $n = 2$, and some enhancement was observed only for heavy ($n = 20, 24$) clusters. No magic numbers below $n = 10$ were observed in the He discharge seeded with H_2O [41] and in the field ionization of expanding water vapor [51].

Schindler et al. [56], in studies of IR radiation-induced decay of heavy cations formed in the ultrasonic water vapor expansion, reported magic numbers $n = 21, 55$. In their experiment, the heavy clusters decay spontaneously because of the ambient infrared radiation, and the $\text{H}^+(\text{H}_2\text{O})_4$ cation was reported as a final stable product.

We note that this ambiguity in the observation of magic numbers for light cations reflects the ways of clusters formation. Magic numbers are well visible in experiments in which the clusters are formed in the step-by-step adding of water molecules to some precursor ions, as in this experiment and those of [8,35,53] or in the decay of heavier ionized clusters [24,56]. Magic numbers are also seen if ions are produced from condensed phases [30,39]. Little, if any, evidence of magic numbers for small clusters comes from experiments in which neutral clusters formed previously in the gas phase are subsequently ionised [17,25,27]. A comparative modeling (see previous) shows that this duality can be caused by different geometrical structures of ionized and neutral clusters.

5. Experimental binding energies

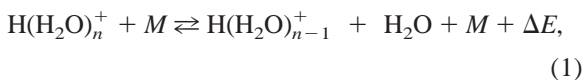
Experimental binding energies for $\text{H}^+(\text{H}_2\text{O})_n$ clusters have been reviewed in numerous works [38,42–44,58], but independent measurements come only from a few laboratories. Two classes of experiments are to be distinguished. In the first one, the “thermodynamic” method [35,37,38,42–46], enthalpies

$\Delta H_{n-1,n}$ of formation of the n cluster from the $n - 1$ one are evaluated from relative ion abundances versus temperature. Water vapor partial pressures in the 1–100-Pa range are used, as are total gas pressures up to 1000 Pa and temperatures up to 900 °C [37]. The main cause of discrepancies in this type of experiments (e.g. [37] vs. [45]) are nonequilibrium conditions in the ion source (cf. the data in Table 1[a]).

The second category of experiments can be defined as “single-collision” events. Clusters dissociate impact with other molecules [59–62] or with photons [55]; the binding energies are determined from the thresholds of these processes. In particular, binding energies for clusters from $n = 6$ to $n = 28$ were obtained from the photoionization of hydrated methyl iodide molecules [55] and, for $n = 2-4$, from the charge transfer between $\text{H}^+(\text{H}_2\text{O})_n$ and CH_3CN [59,60]. The data of Castelman and coworkers [55,59,60] are somewhat higher than the thermodynamic values [37,38], see Table 1(a). In particular, the most recent $n = 2$ values determined from thresholds for three different charge-transfer reactions diverge by as much as 20% [60].

The photodissociation technique of pure water clusters was used by Magnera et al. [30,31], who obtained binding energies for $n = 2-28$ clusters. The measured values depended somewhat on the number of water molecules detached by the photon impact; generally, the values of Magnera et al. [31] agree with thermodynamic values [37,44] up to $n = 4$ but are lower for higher n .

As the main goal of this work was to study the ion abundances in the presence of an electrical field, the normalization of the population curves to the values of the reduced electrical field prompts us for a rough evaluation of binding energies. We note that in these experiments, at reduced fields >350 Td, only two types of clusters are observed (see Fig. 3). For the E/N values at which the n and $n - 1$ abundances are equal, one can assume thermodynamic equilibrium conditions for the collisional process:



where M is a third body (most probably another water molecule). The energy ΔE necessary for the dissoci-

ation comes both from the thermal motion of the cluster and M body and from the kinetic energy acquired by the cluster in the electrical field, the latter one dominating. Note that reaction (1) is a two-body dissociation in the forward direction and a three-body attachment in the reverse direction. An exact analysis of its kinetics would require a statistical analysis of all possible reactions in the swarm, therefore exceeding the scope of this article.

Some difficulty in the evaluation of ΔE in the swarm experiment comes from the indetermination of the energy acquired by the ion from the electric field. The mean free path λ of the cluster between two collisions with water molecules can be obtained from the following expression:

$$\lambda N = \frac{4}{\pi(d_1 + d_2)^2}, \quad (2)$$

where d_1 and d_2 are diameters of the two colliding bodies (water molecule and the cluster), and N is the water vapor density. For the water molecule diameter, we adopted the value of $d_1 = 2.9 \times 10^{-10}$ m obtained from experimental van der Waals parameters [63]. The choice of a van der Waals radius is justified, as our pressure values are not far from the vapor saturation conditions at 300 K. We assume also that the diameters d_2 scale as $n^{1/3}$, with the number of water molecules in the cluster, for example, the equivalent diameter of $\text{H}^+(\text{H}_2\text{O})_2$ is $3\sqrt{2}$ times d_1 .

Using these assumptions, we evaluate the collisional energy in Eq. (1) in the laboratory system from the formula

$$\Delta E = 3kT + q(E/N)_0(\lambda N), \quad (3)$$

where q is the cluster charge and $(E/N)_0$ the value of the reduced field at which the n and $n - 1$ abundances are in a mutual equilibrium. In formula (3), the factor $3kT$ takes into account the translational energy caused by the thermal motion ($3/2kT$) and by the rotational energy of colliding particles ($3/2kT$).

Although, at fields <350 Td, several different clusters coexist at the same value of the reduced field, we extend our analysis also to these conditions, obtaining the dissociation energies $E_{n-1,n}$ of the

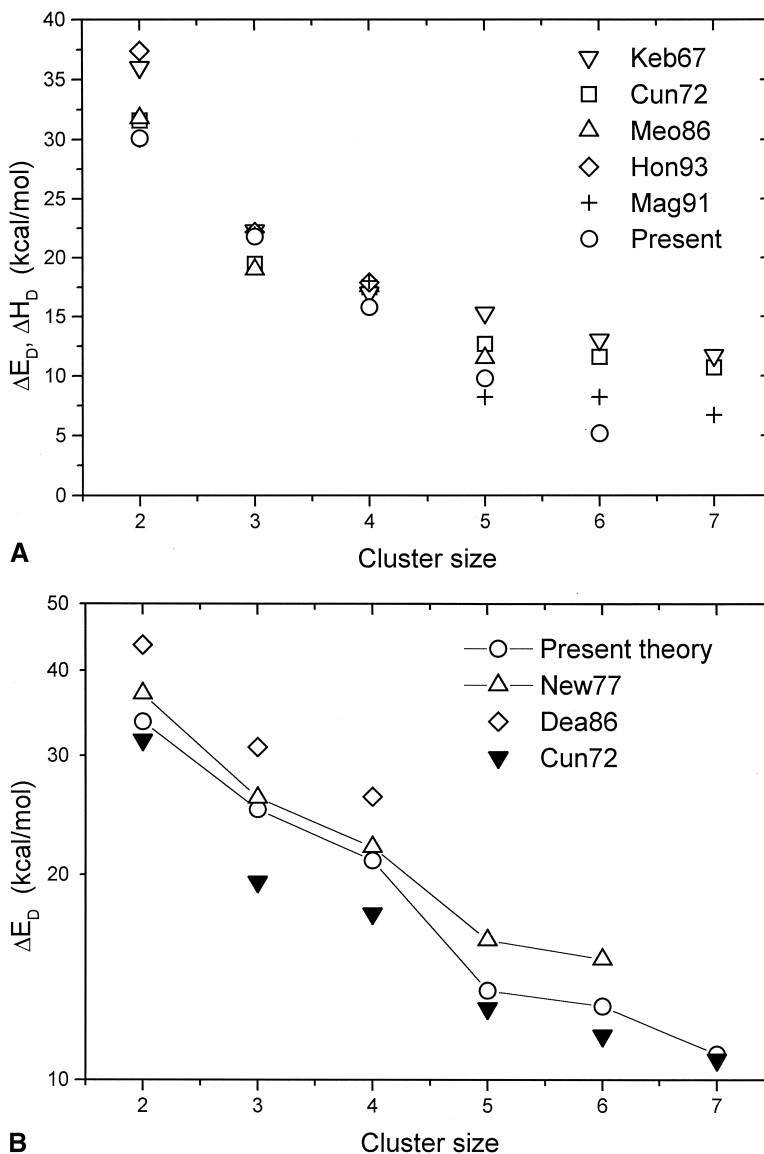


Fig. 4. Dissociation energy for the process $\text{H}(\text{H}_2\text{O})_n^+ \rightleftharpoons \text{H}(\text{H}_2\text{O})_{n-1}^+ + \text{H}_2\text{O} + \Delta E$ as function of cluster size n . *a*, Experimental data: thermodynamic equilibria, Keb67 [35], Cun72 [37] and [38], Meo86 [44]; single-collision thresholds, Hon93 [60] charge transfer with CH_3CN ; Mag91 [31] photodissociation; present, evaluation from relative abundances. *b*, Theory (Hartree-Fock): New77 [57], 4-31G; Dea86 [66] 3-21G/4-31G; present, calculations in 6-311G** basis set; Cun72 [37,38] experimental.

clusters from the intersection points of relative abundances for n and $n - 1$ clusters. Our estimate of the statistical error in this evaluation that comes from the uncertainty of experimental conditions (pressure, temperature), from fitting procedures, and from the noise in relative abundances is $\sim 15\%$.

Values of $E_{n-1,n}$ from the present analysis are shown in Fig. 4 and in Table 1(a). Generally, the present data up to $n = 5$ fall within the overall determinations from other methods (see Fig. 4[a]). Present dissociation energies for clusters $n = 2, 3, 4$ agree well with the more recent enthalpies of forma-

tion obtained in thermodynamic experiments [37,44], the discrepancies being within 10%. The present dissociation energy for $n = 2$ is somewhat lower than the result from the recent single-collision experiment [60] but agrees very well with it for $n = 3$ (see Table 1[a]). Unfortunately, no dissociation energies for clusters with $n > 4$ were obtained in [60].

As for clusters up to $n = 5$, the agreement between present results and other experiments, in particular with [44], is pretty good; our dissociation energy of the $n = 6$ cluster is surely underestimated. This value is not only lower than other experimental determinations but does not follow the trend pointed out by several authors [35,43,64], according to which the dissociation $E_{n-1,n}$ energies for higher n should approach the enthalpy of solvation in the liquid phase (10.5 kcal/mole for H_2O). The present error is surely of a different nature than discrepancies between some thermodynamic data [37,45] (cf. in Table 1).

As stated above, a big uncertainty comes from the estimate of the free path between subsequent collisions. The choice of scaling d_2 with $n^{1/3}$ and the use of van der Waals hard-sphere radius for d_1 are obviously the simplest choices. By structural modeling (see below); we have verified that the $n^{1/3}$ scaling holds pretty well; the calculated equivalent radius of the $\text{H}^+(\text{H}_2\text{O})_6$ cluster is lower than the one calculated from the $n^{1/3}$ scaling of the theoretical H_2O radius by merely 1%. However, we have not used the theoretical radii because the calculated H_2O diameter (3.18×10^{-10} m) is somewhat different than the experimental van der Waals value.

The present evaluation of the free path disregards also the attractive interaction between the charged cluster and the dipole moment of the H_2O molecule; the capture radius for such an interaction is independent of the cluster size [65]. The use of a constant radius of interaction would improve the agreement at higher n , but it is not fully justified.

From the experimental side, the influence of possible other systematic errors on measurements, as, for example, contact potentials or residual penetration of the electrical field from the discharge into the drift cell, are not to be excluded. At the lowest voltages applied (i.e., in the studies of heavier clusters), this

effect can cause underestimation of binding energies. An improvement of present measurements for $n = 6$ would require, first of all, a better separation of the drift chamber from stray electrical fields.

As noted before, determining the fragmentation energy in our experiment from the intersection of n and $n - 1$ curves is a rather rough approximation for high n , where several types of clusters coexist for the same E/N values (see Fig. 3). A more precise modeling of the collisional dissociation, taking into account coexistence of different clusters, should be performed. We note, for example, that the $\text{H}^+(\text{H}_2\text{O})_3 \rightleftharpoons \text{H}^+(\text{H}_2\text{O}) + 2\text{H}_2\text{O}$ process, observed by Honma et al. [60], occurs at certain collision energies with a probability only a little smaller than that for the $\text{H}^+(\text{H}_2\text{O})_3 \rightleftharpoons \text{H}^+(\text{H}_2\text{O})_2 + \text{H}_2\text{O}$ reaction.

We note, finally, that the exact measured quantity in our experiment is the activation energy for the decomposition in three body collisions. As noted by Meot-Ner and Field [42] for the $\text{H}(\text{H}_2\text{O})_2^+$ decomposition, the rate constant of this reaction depends strongly on the temperature, so the activation energy can be by a few kcal/mole lower than the enthalpy of formation of the cluster. For $\text{H}(\text{H}_2\text{O})_2^+$, the activation energy for the decomposition is 29.8 kcal/mole, compared to 33.0 kcal/mole reported for $\Delta H_{n-1,n}$ [42]. Although the reported difference between $\Delta H_{n-1,n}$ and $\Delta E_{n-1,n}$ is < 1 kcal/mole in the case of $n = 6$ [55], the measurements of dissociation energies [30,31,55,59] seem to be more appropriate for comparison with the present data. We recall that present dissociation energies for all clusters but $n = 6$ agree reasonably well with the measurements by Magnera et al. [31] in pure water vapor.

6. Comparative modeling

Recent ab initio calculations on water neutral clusters show a high level of confidence, allowing us to model many different configurations of $(\text{H}_2\text{O})_n$ with $n = 3-8$ [20–22,40,50]. From these works, it follows that neutral clusters tend to form closed structures in the lowest-energy state, such as a close ring [20,30] for the trimer or a form of the book with

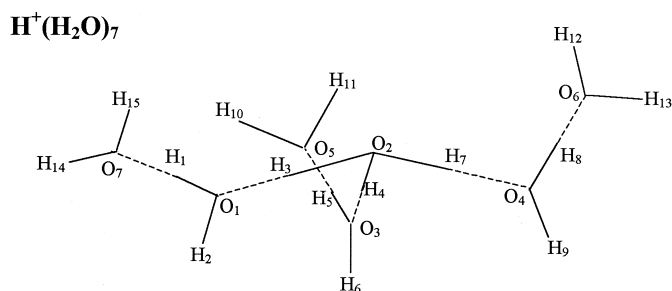


Fig. 5. Geometrical configuration of cationic water heptamer, present calculations.

two “pages” for the heptamer [21]. For charged clusters, the expected geometries differ from those of neutral species [16,22]. In spite of numerous calculations, we are aware of only fragmentary data for dissociation energies for cations; these energies were calculated in extended molecular orbital basis sets either for few clusters [46] or for more clusters but in low sets [57,66]. Finally, in many works the geometries are modeled but no binding energies were reported [18,19,22].

At present, the HyperChem 5.0 software packet in the self-consistent-field Hartree-Fock approximation, exploiting four molecular orbital basis sets, 3-21G, 4-31G, 6-31G**, and 6-311G**, has been used. The method has been tested for the neutral water trimer configuration in the 6-31G** splitted-valence molecular-orbital basis set with two polarization functions (d, p). The obtained geometrical parameters agree within 2% with the recent Møller-Plesset results in the augmented correlation-consistent basis set [20]. The presently calculated linear configuration of the neutral trimer has the total energy higher by 6.6 kcal/mole than the closed structure.

Several geometries, linear, isomeric, and closed, were exploited for the whole $n = 1-7$ cations series. We maintained the requirement of successive growing of clusters, that is, the n -th cluster is obtained from the $(n - 1)$ th cluster by adding one water molecule without changing the existing bonds. Details of the obtained configurations will be given separately [67]. In Fig. 5, we show the geometry of the lowest-energy configurations for the $\text{H}^+(\text{H}_2\text{O})_7$ clusters. As seen from the figure, the basic structure of the cluster is the Eigen’s [3] asterisk-like tetramer, composed of three

water molecules attached via hydrogen bonds to the H_3O^+ ion core. Present geometries for n up to 6 are similar to those in [57]. The Eigen’s tetramer base remains the same for the whole $n = 1-7$ series. The closed and linear geometries of the $n = 4$ cluster, for example, have total energies 4.9 and 5.0 kcal/mol higher than the Eigen’s structure; for $n = 6$, the energetically closest isomer lies only 0.35 kcal/mol higher than our lowest configuration [67].

The dissociation energies of the lowest-energy configurations obtained in the 4-31G, 6-31G**, and 6-311G** basis sets are given in Table 1(b). The energy of proton hydration ($-\Delta E = 178.8$ kcal/mole) is slightly higher than that obtained by Frisch [68] and Newton [57]. Energies of dissociation up to $n = 5$ coincide in the 6-31G** and 6-311G** basis sets, indicating in particular slightly enhanced stability of the $n = 4$ cluster (see Fig. 4[b]). For $n = 6, 7$, the 6-311G** data deviate somewhat from those in the 6-31G** basis set. The 6-311G** calculation predicts a little bit smoother variation of ΔE between $n = 5, 7$ than does the 6-31G** basis set (cf. in Table 1[b]). We recall that for $n = 6$, we observed experimentally only slightly enhanced relative abundances, while for $n = 4$, the effect was quite clear (see Fig. 3).

Present dissociation energies are in the good agreement with thermodynamic data [37,38,44] for $n = 2$ and $n = 5-7$, especially if the zero-vibration correction in the theoretical data would be performed. Such a correction for $n = 2$ clusters, +1.1 kcal/mole [18], brings the present theoretical value to coincidence with the thermodynamic measurements [37,44]. For $n = 3$ and 4, the theoretical values are higher than the

thermodynamic ones [37,44]; for $n = 2$ being closer to the present and the single-collision [31,60] experiments, compare Table 1(a) and Table 1(b). In the whole $n = 2-7$ range, the present theory lies closer to the experimental values [37,38] than do the calculation of Newton [57] (see Fig. 4[b]). Both the present and Newton's models [57] show some discontinuity between $n = 4$ and $n = 5$ binding energies.

We have also repeated calculations of Deakney [66] performed with a 3-21G/4-31G basis set for $n = 1-4$ cationic clusters—confirming his $\Delta E_{n-1,n}$ is within 1% (see Table 1[b]). Note that the dissociation energies of Newton [57] obtained in the 4-31G basis set are somewhat lower than the present 4-31G ones for the semiempirical zero-energy correction included in [57]. The calculated dissociation energy falls with including higher molecular orbitals; for example, for the $n = 4$ cation from 29.0 to 25.8 and 20.3 kcal/mol, changing the basis sets from 3-21G to 4-31G and 6-31G**, respectively. It was shown by Frisch et al. [68] for the $n = 2$ clusters that farther expanding of the orbital base, from 6-31G* (d, p) to 6-311**G(3df, 3pd), changes only little the dissociation energy, from 35.3 to 34.8 kcal/mole. We checked also that the low, 3-21G base used in [66] gives a wrong, planar configuration of the H_3O^+ ion, which is a pyramidal one in the 6-31G** calculations.

Present comparative calculations show that geometrical configurations of small neutral and ionized clusters are different: Closed for the first class and star-like for the second one. This result is independent of the molecular orbitals basis set used. Therefore, in the ionization processes of already formed neutral clusters, some rearranging of the configuration is necessary to obtain the lowest energy state. As far as proton remains mobile inside small clusters [22,69] and the differences between binding energies of isomers are small, thus facilitating the rearrangement, the measured abundances may be subject to changes.

7. Conclusions

A swarm-like experiment has been performed on water clusters at room temperature and pressures in a

few Torr range. The present measurements introduce a new element into studies of water vapor clusters, namely, an external electrical field. In our set-up, the water ions and/or cluster ions formed in the electrical discharge collide with neutral water molecules in the drift chamber and form and/or disintegrate into other agglomerates. A wide range of small positively charged clusters $\text{H}^+(\text{H}_2\text{O})_n$ with $n = 1-7$ was observed, similar to the early experiment by Kebarle et al. [35]. Relative populations of clusters in the present experiment are governed by the values of the reduced electric field. Our data evidence relatively higher abundances for the $n = 4$ cluster.

We propose a method for a rough estimate of the dissociation energies of light clusters; the present results fall into the overall spread of recent measurements. Unfortunately, our work does not clarify existing discrepancies between the thermodynamic [35,37,38,66,67] and collisional [59,60] determinations of the binding energies. The present data are somewhat closer to another determination of dissociation energies in a pure water environment using photons as projectiles [30,31] than to the experiments involving mixed clusters (with CH_3I [55] or CH_3CN [59]). The present theoretical dissociation energies agree well with thermodynamic determinations [37,38] and reasonably well with previous theoretical values [57] obtained for the $n = 1-6$ series.

In conclusion, an experiment is presented in which a whole class of light cationic water clusters, corresponding to the filling up of the first and second shell around H_3O^+ [3], can be easily observed. Relative abundances of clusters are controlled by the electrical field applied. A way of evaluating the dissociation energies of clusters, methodologically between the thermodynamic [35–38,42–46] and single-collision experiments [30,31,59,60], is proposed.

Acknowledgments

We acknowledge substantial support from Prof. Olgierd Gzowski, who made this work possible. We thank also one of the referees who indicated to us a way of improving the theoretical approach.

References

- [1] C.H. Cho, S. Singh, G.W. Robinson, *Phys. Rev. Lett.* 76 (1996) 1651.
- [2] P. Jedlovszky, R. Vallauri, *Mol. Phys. Lett.* 97 (1999) 1157.
- [3] M. Eigen, L. de Maeyer, *Proceedings of the Royal Society of London A* 247 (1958) 505.
- [4] M. Eigen, *Angew. Chem.* 75 (1963) 489.
- [5] L. Degréve, C. Quintale, Jr., *J. Chem. Phys.* 101 (1994) 2319.
- [6] P.F. Knewstubb, A.W. Tickner, *J. Chem. Phys.* 38 (1963) 464.
- [7] P. Kebarle, E.W. Godbole, *J. Chem. Phys.* 39 (1963) 1131.
- [8] A. Good, D.A. Durden, P. Kebarle, *J. Chem. Phys.* 52 (1970) 212, 222.
- [9] H.R. Carlon, *J. Appl. Phys.* 52 (1981) 1584.
- [10] R.S. Narcisi, A.D. Bailey, *J. Geophys. Res.* 70 (1965) 3787.
- [11] E. Arijis, D. Nevejans, J. Ingels, *Int. J. Mass Spectrom. Ion Processes* 81 (1987) 15.
- [12] I. Kusaka, Z.-G. Wang, J.H. Seinfeld, *J. Chem. Phys.* 102 (1995) 913, 8993.
- [13] G. Hauck, F. Arnold, *Nature* 311 (1984) 547.
- [14] H. Ziereis, F. Arnold, *Nature* 321 (1986) 503.
- [15] A. Hansel, W. Singer, A. Wisthaler, M. Schwarzmann, W. Lindinger, *Int. J. Mass Spectrom. Ion Processes* 167/168 (1997) 697.
- [16] L.I. Yeh, M. Okumura, J.D. Myers, J.M. Price, Y.T. Lee, *J. Chem. Phys.* 91 (1989) 7319; L.I. Yeh, Y.T. Lee, J.T. Hougen, *J. Mol. Spectrosc.* 164 (1994) 473.
- [17] O. Björneholm, F. Federmann, S. Kakar, T. Möller, *J. Chem. Phys.* 111 (1999) 546.
- [18] Y. Xie, R.B. Remington, H.F. Schaefer III, *J. Chem. Phys.* 101 (1994) 4878; E.F. Valeev, H.F. Schaefer III, *J. Chem. Phys.* 108 (1998) 7197.
- [19] D. Wei, D.R. Salahub, *J. Chem. Phys.* 101 (1994) 7633; D. Wei, D.R. Salahub, *J. Chem. Phys.* 106 (1997) 6086.
- [20] I.M.B. Nielsen, A.T. Seidl, C.L. Janssen, *J. Chem. Phys.* 110 (1999) 9435.
- [21] J. Kim, D. Majumdar, H.M. Lee, K.S. Kim, *J. Chem. Phys.* 110 (1999) 9128; J. Rodriguez, D. Laria, E.J. Marceca, D.A. Estrin, *J. Chem. Phys.* 110 (1999) 9039.
- [22] C.V. Ciobanu, L. Ojamäe, I. Shaviit, S.J. Singer, *J. Chem. Phys.* 113 (2000) 5321.
- [23] J.Q. Searcy, J.B. Fenn, *J. Chem. Phys.* 61 (1974) 5282.
- [24] C. Berg, U. Achatz, M. Beyer, S. Joos, G. Albert, T. Schindler, G. Niedner-Schatteburg, V.E. Bondybey, *Int. J. Mass Spectrom. Ion Processes* 167/168 (1997) 723.
- [25] V. Hermann, B.D. Kay, A.W. Castleman, Jr., *J. Chem. Phys.* 72 (1982) 185.
- [26] M. Tsuchiya, E. Aoki, H. Kuwabara, *Int. J. Mass Spectrom. Ion Processes* 90 (1989) 55.
- [27] P.P. Radi, P. Beaud, D. Franzke, H.-M. Frey, T. Gerber, B. Mischler, A.-P. Tzannis, *J. Chem. Phys.* 111 (1999) 512.
- [28] H. Haberland, C. Ludewigt, H.-G. Schindler, D.R. Worsnop, *J. Chem. Phys.* 81 (1984) 3742.
- [29] M. Lancaster, F. Honda, Y. Fukuda, J.W. Rabelais, *J. Am. Chem. Soc.* 101 (1979) 1951.
- [30] T.F. Magnera, D.E. David, D. Stulik, R.G. Orth, H.T. Jonkman, J. Michl, *J. Am. Chem. Soc.* 111 (1989) 5036.
- [31] F. Magnera, D.E. David, J. Michl, *Chem. Phys. Lett.* 182 (1991) 363.
- [32] E.A. Mason, E.W. McDaniel, *Transport properties of ions in gases*, Wiley-Interscience, New York (1988).
- [33] T. Wróblewski, E. Gazda, 6th EPS Conference on Atomic and Molecular Physics, Siena, Contributed Papers; Vol. 22D (1998), pp. 9–30; T. Wróblewski and E. Gazda, The XXIVth International Conference on Phenomena in Ionized Gases, Warsaw, Abstracts, Vol. IV (1999) p. 121.
- [34] E. Gazda, *J. Phys. B* 19 (1986) 2973.
- [35] P. Kebarle, S.K. Searles, A. Zolla, J. Scarborough, M. Arshadi, *J. Am. Chem. Soc.* 89 (1967) 6393.
- [36] M. DePaz, J.J. Lewenthal, L. Friedman, *J. Chem. Phys.* 51 (1969) 3748.
- [37] A.J. Cunningham, J.D. Payzant, P. Kebarle, *J. Am. Chem. Soc.* 1 (1972) 7627.
- [38] Y.K. Lau, S. Ikuta, P. Kebarle, *J. Am. Chem. Soc.* 104 (1982) 1462.
- [39] S.A. McLuckey, G.L. Glish, K.G. Asano, J.E. Bartmess, *Int. J. Mass Spectrom. Ion Processes* 109 (1991) 171.
- [40] D. Kreisler, O. Echt, M. Knapp, E. Recknagel, *Surf. Sci.* 156 (1985) 321.
- [41] X. Yang, X. Zhang, A.W. Castleman, Jr., *Int. J. Mass Spectrom. Ion Processes* 109 (1991) 339.
- [42] M. Meot-Ner, F.H. Field, *J. Am. Chem. Soc.* 99 (1977) 998.
- [43] M. Meot-Ner (Mautner), *J. Am. Chem. Soc.* 106 (1984) 1625.
- [44] M. Meot-Ner (Mautner), C.V. Speller, *J. Phys. Chem.* 90 (1986) 6616.
- [45] D.P. Beggs, F.H. Field, *J. Am. Chem. Soc.* 93 (1971) 1567, 1576.
- [46] K. Hiraoka, H. Takimoto, S. Yamabe, *J. Chem. Phys.* 90 (1986) 5910.
- [47] F. Howorka, W. Lindinger, R.N. Varney, *J. Chem. Phys.* 61 (1974) 1180.
- [48] J. Mechińska-Drewko, W. Roznerski, Z. Lj. Petrović, G.P. Karwasz, *J. Appl. Phys.* 32 (1999) 2746.
- [49] M. Knapp, O. Echt, D. Kreisler, E. Recknagel, *J. Chem. Phys.* 85 (1986) 636.
- [50] J. Kim, I. Becker, O. Cheshnovsky, M.A. Johnson, *Chem. Phys. Lett.* 297 (1998) 90.
- [51] R.J. Beuhler, L. Friedman, *J. Chem. Phys.* 77 (1982) 2549.
- [52] K. Hiraoka, K. Morise, T. Shoda, *Int. J. Mass Spectrom. Ion Processes* 67 (1985) 11.
- [53] L. Poth, Z. Shi, Q. Zhong, A.W. Castleman, Jr., *Int. J. Mass Spectrom. Ion Processes* 154 (1996) 35.
- [54] D. Dreyfuss, H.Y. Wachman, *J. Chem. Phys.* 76 (1982) 2031.
- [55] Z. Shi, J.V. Ford, S. Wei, A.W. Castleman, Jr., *J. Chem. Phys.* 99 (1993) 8009.
- [56] T. Schindler, C. Berg, G. Niedner-Schatteburg, V.E. Bondybey, *Chem. Phys. Lett.* 229 (1994) 57.
- [57] M.D. Newton, *J. Chem. Phys.* 67 (1977) 5535.
- [58] R.G. Keesee, A.W. Castleman, Jr., *J. Phys. Chem. Ref. Data* 15 (1986) 1011.
- [59] K. Honma, L.S. Sunderlin, P.D. Armentrout, *Int. J. Mass Spectrom. Ion Processes* 117 (1992) 237.
- [60] K. Honma, L.S. Sunderlin, A.W. Castleman, Jr., *J. Chem. Phys.* 99 (1993) 1623.

- [61] X. Yang, A.W. Castelman, Jr., *J. Chem. Phys.* 95 (1991) 130.
- [62] A.A. Viaggiano, F. Dale, J.F. Paulson, *J. Chem. Phys.* 88 (1988) 2469.
- [63] S. Dushman, *Scientific foundations of vacuum technique*, Wiley, New York (1962).
- [64] A.W. Castelman, Jr., R.G. Keesee, *Science* 241 (1988) 36.
- [65] W.J. Chesnavich, T. Su, M.T. Bowers, *J. Chem. Phys.* 72 (1980) 2641.
- [66] C.A. Deakayne, M. Meot-Ner (Mautner), C.L. Campbell, M.G. Hughes, S.P. Murphy, *J. Chem. Phys.* 84 (1986) 4958.
- [67] T. Wróblewski, G.P. Karwasz, *Sci. Rep. Stupsk Univ.* 14a (2001) in print.
- [68] M.J. Frisch, J.E. Del Bene, J.S. Binkley, H.F. Schaefer III, *J. Chem. Phys.* 84 (1986) 2279.
- [69] M. Henchman, D. Smith, N.G. Adams, *Int. J. Mass Spectrom. Ion Processes* 109 (1991) 105.